Large-Grain Polycrystalline Silicon Films Formed through Flash-Lamp-Induced Explosive Crystallization

Keisuke Ohdaira[1,2,*], Keisuke Sawada[1], Noritaka Usami[3], Sergey Varlamov[4], and Hideki Matsumura[1]

[1]Japan Advanced Institute of Science and Technology,

Nomi, Ishikawa 923-1292, Japan

[*]E-mail address: ohdaira@jaist.ac.jp

[2]PRESTO, Japan Science and Technology Agency,

Kawaguchi, Saitama 332-0012, Japan

[3]Institute for Materials Research, Tohoku University,

Sendai, Miyagi 980-8577, Japan

[4]University of New South Wales, Sydney, NSW 2052, Australia

The flash lamp annealing (FLA) of electron-beam- (EB-) evaporated amorphous silicon (a-Si) films results in the formation of polycrystalline Si (poly-Si) films with at least a few μm long grains stretching along lateral crystallization directions. Unlike the case of using chemical-vapor-deposited (CVD) hydrogenated a-Si films as precursors, no peeling of Si films occurs even in the absence of Cr adhesion layers. Such a flash-lamp-induced crystallization occurs also in doped EB-evaporated a-Si films as in the case of undoped films. The $p^+/p^-/n^+$ stacked structure is sufficiently kept even after crystallization, although the profiles of dopants are slightly modified. This fact clearly indicates that the crystallization observed is not based on liquid-phase epitaxy (LPE)

after the complete melting of the whole a-Si precursor during millisecond-order treatment but through LPE-based explosive crystallization (EC), self-catalytic lateral crystallization driven by the release of latent heat. The formation of poly-Si films with large grains and the sufficient preservation of dopant profiles would lead to the utilization of the poly-Si films formed for solar cell devices.

1. Introduction

Bulk crystalline silicon (c-Si) solar cells occupy a current photovoltaic market share of more than 80% because of their high conversion efficiency and matured production processes. The fabrication cost of bulk c-Si solar cells, however, has not been fully reduced mainly owing to the large amount of Si material usage. To overcome this issue, the utilization of thin-film c-Si as absorbers has been desired, and the cost-effective method of producing c-Si thin films should be established. CSG solar has demonstrated solar cells with a conversion efficiency of more than 10% fabricated using large-grain polycrystalline Si (poly-Si) films formed through solid-phase crystallization (SPC).[1] Duration required for the SPC is, however, ~10 h or more, which is not acceptable for mass production. Instead of the time-consuming thermal-equilibrium annealing process, rapid annealing processes for the crystallization of precursor a-Si films have been investigated.[2-4] Of a variety of rapid annealing techniques, flash lamp annealing (FLA), in which millisecond-order pulse light from Xe lamps is used,[5-7] can crystallize a-few-μm-thick a-Si films without heating whole glass substrates owing to its proper annealing duration. We have so far succeeded in the formation of 4.5-μm-thick poly-Si films on glass substrates by the FLA of a-Si films.[8,9] The poly-Si films formed contain characteristic periodic microstructures on the surface of and inside the poly-Si films when we use precursor a-Si films formed by catalytic chemical vapor deposition (Cat-CVD) or sputtering,[10,11] resulting from explosive crystallization (EC), lateral crystallization driven by the release of latent heat.[12] The particular poly-Si films consist of 10-nm-sized fine grains as well as 100-nm-sized relatively large grains. On the contrary, the FLA of electron-beam- (EB-) evaporated a-Si films results in the formation of poly-Si films with larger grains with sizes of at

least a few μm.[13,14] In this study, we have characterized flash-lamp-crystallized (FLC) poly-Si films formed from EB-evaporated a-Si films in detail. Furthermore, in order to utilize the large-grain poly-Si films as solar cell materials, we have attempted to perform the FLA of stacked $n^+/p^-/p^+$ a-Si films mainly formed through EB evaporation. We have confirmed that doped EB-evaporated films can be crystallized by a mechanism similar to undoped EB films, and dopant profiles can be sufficiently kept even after LPE-based EC so that the $n^+/p^-/p^+$ poly-Si structure can be utilized for solar cells.

2. Experimental Procedure

We first prepared two kinds of precursor a-Si film structures: (i) ~2-μm-thick undoped EB-evaporated a-Si films and (ii) $p^+/p^-/n^+$ stacked a-Si films consisting of 100-nm-thick B-doped (2.5×10^{19} cm^{-3}) EB-evaporated a-Si, 2-μm-thick B-doped (3×10^{16} cm^{-3}) EB-evaporated a-Si, and 35-nm-thick P-doped (1.7×10^{20} cm^{-3}) plasma-enhanced CVD (PECVD) dehydrogenated a-Si, both of which were formed directly on Corning Eagle glass substrates. FLA was performed using pulse light at a fluence of ~15 J/cm^2 with 5-8 ms duration in Ar atmosphere with the preheating of samples at 500 °C. Only one shot of flash lamp irradiation was performed for each sample. We used a multi-pulse FLA system in this study, instead of a conventional single-pulse FLA system, in order to evaluate lateral EC velocity.[13] The emission of sub-pulses, tunable in the range of 1-10 kHz, leads to the periodic modulation of the temperature of a Si film, resulting in the formation of macroscopic stripe patterns. The width of stripe patterns and sub-pulse emission frequency yield EC velocity.[13] The poly-Si films formed were characterized by Raman spectroscopy, electron backscatter diffraction (EBSD), and cross-sectional transmission electron microscopy (TEM). We

also performed secondary ion mass spectrometry (SIMS) to check dopant profiles in poly-Si films formed from $p^+/p^-/n^+$ stacked a-Si films.

3. Results and Discussion

Figure 1 shows a surface image and a Raman spectrum of a FLC poly-Si film formed from an undoped EB-evaporated a-Si film. One can see the signatures of lateral crystallization and stripe patterns formed owing to the emission of discrete sub-pulses. The full width at half maximum (FWHM) of the c-Si peak at ~520 cm^{-1} is ~4.5 cm^{-1}, which is close to that of a reference c-Si wafer of ~4 cm^{-1}, indicating the formation of relatively large grains. EC velocity can be estimated to be ~14 m/s from the width of the macroscopic stripes and sub-pulse emission frequency. This value is close to the liquid-phase epitaxial (LPE) velocity of liquid Si at approximately the melting point of a-Si, that is ~1187 °C.[6] This fact indicates that the crystallization observed here is governed by LPE-based EC. It should also be noted that no Si film peeling occurs even without a Cr adhesion layer between a Si film and a glass substrate, unlike the case of hydrogenated Cat-CVD or PECVD a-Si films.[15] The most likely reason for the suppression of Si film peeling is the absence of a large amount of hydrogen inside EB-evaporated a-Si films. We have observed no peeling of sputtered a-Si films with a small amount of hydrogen atoms and sufficiently dehydrogenated Cat-CVD a-Si films even without Cr adhesion layers.[11,15] This observation clearly indicates that the amount of hydrogen inside precursor a-Si films has a critical role in the peeling of Si films, and the result in EB-evaporated a-Si films is quite consistent with this observation. This superior adhesiveness will contribute to the realization of various kinds of device structures including superstrate-type cells.

Figure 2 shows the EBSD normal direction (ND) and transverse direction (TD) color maps of the surface of a FLC poly-Si film formed from an EB-evaporated a-Si film and corresponding inverse pole figures (IPFs). One can see several tens of μm-long grains on the surface of the poly-Si, which results from LPE-based EC discussed above. According to the ND color maps, surface grains have random orientations, which seems to be contrary to previous X-ray diffraction (XRD) pattern data showing a particular orientation.[14] This might be because EBSD has a much higher surface sensitivity of several tens of nm than XRD using X-ray with much larger penetration depth into c-Si, and underlying grains might be more oriented. The TD color map indicates that preferential LPE directions are (100) and (110) rather than (111). This is probably due to a significantly smaller LPE velocity in (111) direction than those of (100) and (110) directions,[16] and the LPE in (111) direction cannot thus persist even if it is initiated.

Figure 3(a) shows the cross-sectional TEM image of a FLC poly-Si film formed from a $p^+/p^-/n^+$ stacked EB-evaporated a-Si film, whose cross-section was formed along a lateral crystallization direction. We can confirm at least a few μm-long crystal grains stretching along a lateral crystallization direction, and 10-nm-sized fine grains are not seen. These features are completely different from those of FLC films formed from Cat-CVD or sputtered films,[11,12] and quite similar to those of FLC poly-Si films formed from undoped EB-evaporated a-Si films.[13,14] This fact indicates that the doping of impurities at a level of $\sim 10^{16}$ /cm^3 has no significant impact on the EC mechanism. Another interesting point is that there is less significant surface roughness on poly-Si films formed from EB-evaporated a-Si films compared with those formed from Cat-CVD or sputtered a-Si films, as shown in Fig. 3(a). One reason for this fact is the

difference in EC mechanisms. EC with alternating emergence of the solid-phase-nucleation- (SPN-) dominant region and LPE-involved region occurs in the FLA of Cat-CVD or sputtered a-Si films.[11,12] In this EC, compressive stress must be concentrated in the molten regions during the crystallization process, by which a number of periodic surface protrusions are created.[11,12] On the other hand, simple LPE-based EC occurs when we use EB-evaporated a-Si films as precursors, as discussed above as well as in the previous reports.[13,14] In this case, LPE occurs continuously, and excessive stress concentration may be avoided, which could result in a smaller surface roughness. Another possible explanation is the difference in film stress in precursor a-Si films. Cat-CVD and sputtered films have compressive stress, and surface protrusions are formed during EC to relax the compressive stress. On the other hand, EB-evaporated films generally have tensile stress, and the formation of a roughened surface may be suppressed. Figures 3(b) and 3(c) show electron diffraction patterns observed in the p^+ and n^+ regions of the FLC poly-Si film. Clear spot patterns are seen in both images, unlike the case of FLC poly-Si films formed from Cat-CVD or sputtered films showing multi ring patterns, meaning that the crystallization mechanism of the surface and bottom highly doped regions is the same as that of a low-doping-concentration region.

Figure 4 shows SIMS profiles of B and P atoms in the vicinity of the surface and Si/glass interface, respectively, in the FLC poly-Si formed from $p^+/p^-/n^+$ stacked EB-evaporated a-Si films. Although both B and P profiles are slightly broadened compared with initial profiles, the $p^+/p^-/n^+$ structure is sufficiently kept even after crystallization. Since bulk crystalline Si solar cells have much broader doping layers,[17] this suppressed doping profiles indicates the possibility of the utilization of

FLC poly-Si films formed through the simultaneous crystallization of stacked EB-evaporated a-Si films for solar cells. If we consider the crystallization of Si after millisecond-order melting, the diffusion length of dopants (L_D) reaches a few μm and dopant profiles must be completely broken, because of the large diffusion coefficients of B and P in liquid Si on the order of 10^{-4} cm^2/s.[18] The only slight diffusion of dopants during crystallization thus clearly indicates that the crystallization is governed by EC. According to the classical diffusion theory, L_D during the crystallization is roughly estimated to be <50 nm, which corresponds to a melting duration of <100 ns. Since the velocity of EC is 14 m/s, the length of a melted part existing between c-Si and a-Si during EC is roughly ~1 μm, which is one order of magnitude larger than that of values reported previously.[18] This might be due to the overestimation of the diffusion length of dopants. FLC poly-Si films formed from EB-evaporated a-Si films has a number of cracks, as reported previously,[13] probably due to tensile stress that precursor a-Si films originally have. Such cracks could seemingly broaden SIMS profiles, and actual dopant profiles might be much shallower. Another possible reason for the wider melted region is the difference in precursor a-Si thickness. The thickness of a-Si films used in ref. 18 was in the 200-400 nm range, which is about one order of magnitude smaller than that in this study, and a smaller thickness can lead to a narrower melted zone owing to a larger heat loss into a substrate.[19] The larger thickness of ~2 μm of our samples could lead to less heat loss into substrates and might result in a wider melted zone.

Finally, we discuss the feasibility of high-performance solar cells fabricated using FLC poly-Si films formed from EB-evaporated a-Si films. The formation of poly-Si films with large grains and the sufficient preservation of dopant profiles are suitable for

solar cell production. The most significant problem in these poly-Si films is a number of cracks generated during crystallization, as mentioned above. The cause of crack formation is probably tensile stress in precursor a-Si films, and the crack generation would be suppressed by the stress control of precursor films and/or by adding layers covering Si film surface to prevent crack generation.

4. Summary

EB-evaporated a-Si films can be converted to poly-Si films by FLA, with at least a-few-μm-long grains stretching along lateral crystallization directions through LPE-based EC. Si films are not peeled off even without using Cr adhesion films. Doped EB-evaporated a-Si films are crystallized by a mechanism similar to undoped films, and B and P dopant profiles can be fully kept even after LPE-based EC.

Acknowledgements

The authors thank Dr. L. Yang of JAIST for her FLA experiment. We also would like to acknowledge Ulvac Inc. for their provision of a part of EB-evaporated a-Si films. This work was supported by JST PRESTO program.

1) M. J. Keevers, T. L. Young, U. Schubert, and M. A Green: Proc. 22nd European Photovoltaic Solar Energy Conf., 2007, p. 1783

2) S. Janz, S. Reber, H. Habenicht, H. Lautenschlager, and C. Schetter: Conf. Record 4th World Conf. Photovoltaic Energy Conversion (WCPEC), 2006, p. 1403

3) J. K. Saha, K. Haruta, M. Yeo, T. Koabayshi, and H. Shirai: Sol. Energy Mater. Sol.

Cells **93** (2009) 1154.

4) A. A. D. T. Adikaari, N. K. Mudugamuwa, and S. R. P. Silva: Sol. Energy Mater. Sol. Cells **92** (2008) 634.

5) B. Pécz, L. Dobos, D. Panknin, W. Skorupa, C. Lioutas, and N. Vouroutzis: Appl. Surf. Sci. **242** (2005) 185.

6) M. Smith, R. McMahon, M. Voelskow, D. Panknin, and W. Skorupa: J. Cryst. Growth **285** (2005) 249.

7) T. Ito, T. Iinuma, A. Murakoshi, H. Akutsu, K. Suguro, T. Arikado, K. Okumura, M. Yoshioka, T. Owada, Y. Imaoka, H. Murayama, and T. Kusuda: Jpn. J. Appl. Phys. **41** (2002) 2394.

8) K. Ohdaira, Y. Endo, T. Fujiwara, S. Nishizaki, and H. Matsumura: Jpn. J. Appl. Phys. **46** (2007) 7603.

9) K. Ohdaira, T. Fujiwara, Y. Endo, S. Nishizaki, and H. Matsumura: Jpn. J. Appl. Phys. **47** (2008) 8239.

10) K. Ohdaira, S. Ishii, N. Tomura, and H. Matsumura: Jpn. J. Appl. Phys. **50** (2011) 04DP01.

11) K. Ohdaira, S. Ishii, N. Tomura, and H. Matsumura: J. Nanosci. Nanotechnol. **12** (2012) 591.

12) K. Ohdaira, T. Fujiwara, Y. Endo, S. Nishizaki, and H. Matsumura: J. Appl. Phys. **106** (2009) 044907.

13) K. Ohdaira, N. Tomura, S. Ishii, and H. Matsumura: Electrochem. Solid-State Lett. **14** (2011) H372.

14) K. Ohdaira and H. Matsumura: to be published in J. Cryst. Growth [DOI: 10.1016/j.jcrysgro.2011.11.028].

15) K. Ohdaira, K. Shiba, H. Takemoto, T. Fujiwara, Y. Endo, S. Nishizaki, Y. R. Jang, and H. Matsumura: Thin Solid Films **517** (2009) 3472.

16) G. D. Ivlev and E. I. Gatskevich: Appl. Surf. Sci. **143** (1999) 265.

17) T. Janssens, N.E. Posthuma, E. Van Kerschaver, K. Baert, P. Choulat, J. L. Everaert, J. Goosens, W. Vandervorst, and J. Poortmans: Proc. 34th IEEE Photovoltaic Specialists Conf., 2009, p. 878.

18) H. Kodera: Jpn. J. Appl. Phys **2** (1963) 212.

19) H.-D. Geiler, E. Glaser, G. Götz, and M. Wagner, J. Appl. Phys. **59** (1986) 3091.

Figure captions

Figure 1 (a) Surface appearance and (b) Raman spectrum of a FLC poly-Si film formed from an undoped EB-evaporated a-Si film at a sub-pulse emission frequency of 1 kHz. The spectrum of a reference c-Si wafer is also shown in the Raman spectrum.

Figure 2 Surface EBSD ND and TD color maps of a FLC poly-Si film formed from an EB-evaporated a-Si film. Corresponding inverse pole figures are also shown.

Figure 3 (a) Cross-sectional TEM image of a FLC poly-Si film formed from a $p^+/p^-/n^+$ stacked EB-evaporated a-Si film, and electron diffraction patterns in (b) p^+ and (c) n^+ regions.

Figure 4 SIMS profiles of (a) B and (b) P in a FLC poly-Si film formed from a $p^+/p^-/n^+$ stacked EB-evaporated a-Si film.

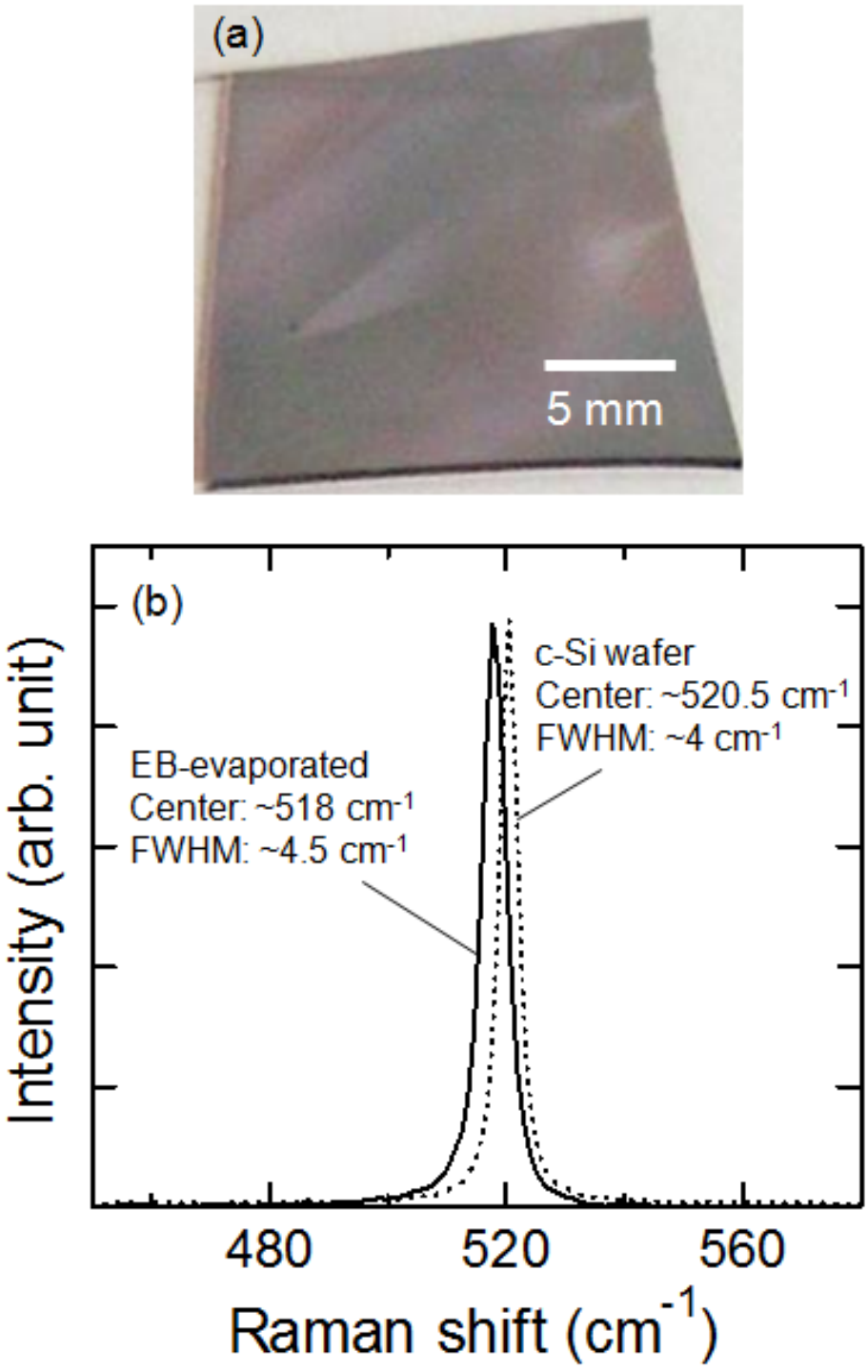

Figure 1 K. Ohdaira *et al*.,

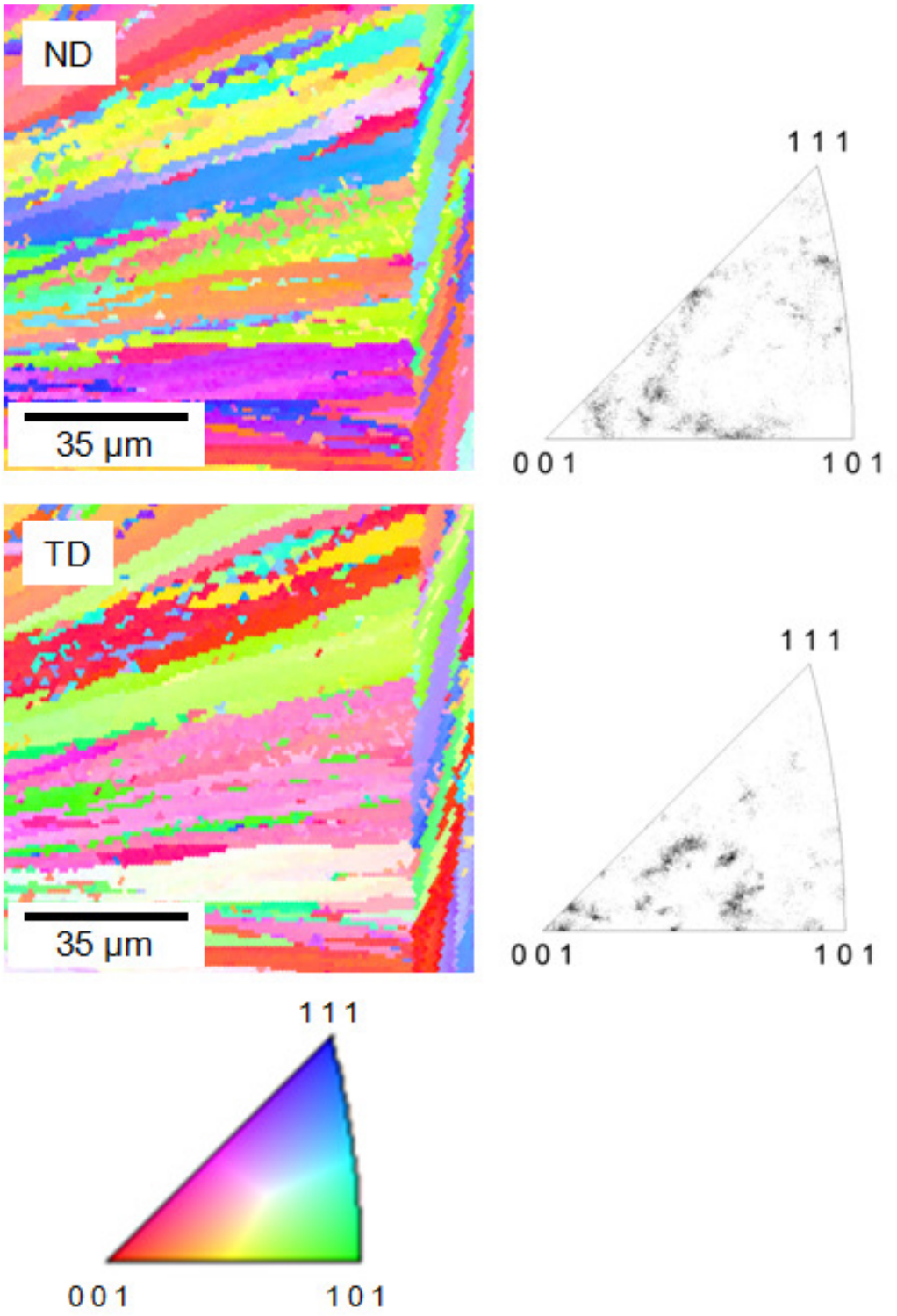

Figure 2 K. Ohdaira *et al*.,

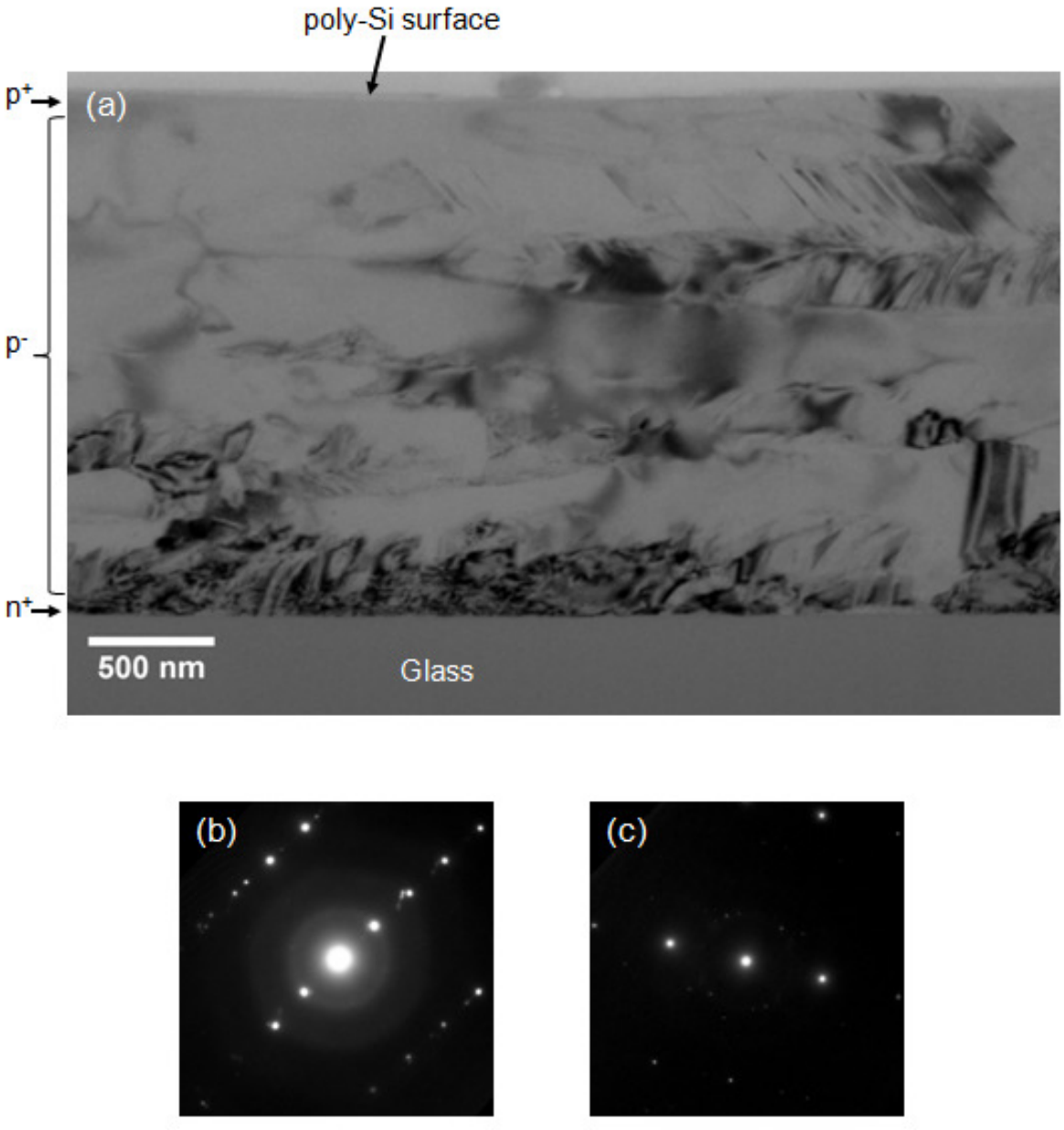

Figure 3 K. Ohdaira *et al*.,

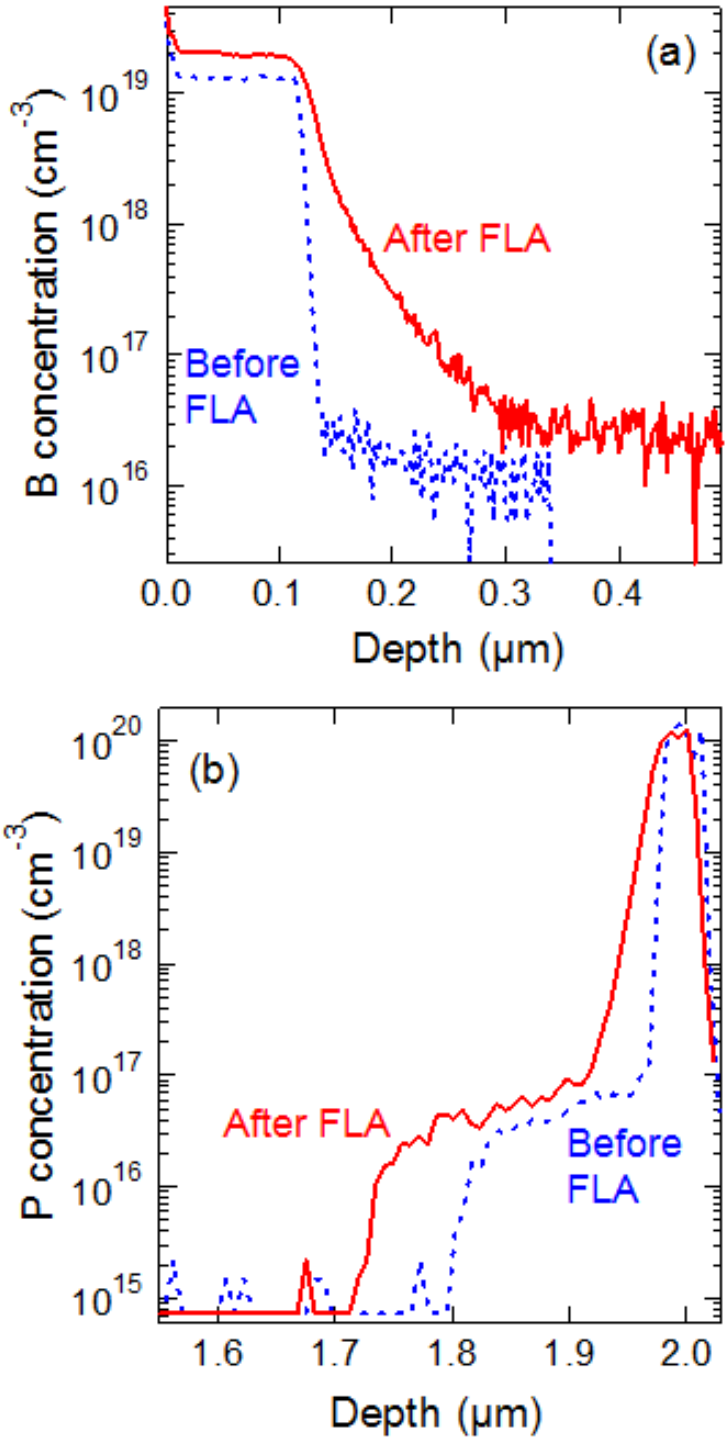

Figure 4 K. Ohdaira *et al*.,